

## Deconvolution of Whole-Core Magnetic Remanence Data by *ABIC* Minimization

Hirokuni ODA<sup>1</sup> and Hidetoshi SHIBUYA<sup>2</sup>

<sup>1</sup>Department of Geology and Mineralogy, Kyoto University, Kyoto 606-1, Japan

<sup>2</sup>Department of Earth Science, CIAS, The University of Osaka Prefecture, Sakai 591, Japan

(Received December 21, 1992; Revised March 14, 1994; Accepted April 15, 1994)

A new, objective deconvolution of whole-core magnetic remanence data is proposed on the basis of Bayesian statistics. The deconvolution is conducted as a smoothness-constrained least squares method with optimum smoothness determined by minimizing a Bayesian Information Criterion (*ABIC*). The deconvolution scheme was applied to whole-core magnetic remanence data of a sediment core measured at intervals of 5 mm. 5-mm-thick specimens were cut from the core to measure the individual magnetizations. These two results showed good agreement in each axis. Synthetic data with different magnitudes of Gaussian noise were also generated; the deconvolution showed more detailed structure with increased signal-to-noise ratio.

### 1. Introduction

The whole-core cryogenic magnetometer was developed to measure the remanent magnetizations of long core samples continuously. The Ocean Drilling Program (ODP) has used such a magnetometer for many years and paleomagnetic remanence data are collected routinely at ten centimeter intervals down-core. In spite of the efficiency of the whole-core measurement, the output signal is not the direct value of the magnetization but the integral of the magnetization by the broad sensor responses. Deconvolution is necessary to reveal variations shorter than the spacial resolution of the sensor responses.

The difficulty is that deconvolution is easily affected by high frequency noise in the data. In frequency space, deconvolution is achieved by dividing the data by the sensor response in each frequency component. As the sensor response function is smooth and the higher frequency components are low, the high frequency noise in the data is easily exaggerated through deconvolution. Thus, we have to reduce the higher frequency noise to get a meaningful solution.

The first attempt to deconvolve whole-core paleomagnetic data was made by Dodson *et al.* (1974). They measured the magnetic remanence of a 1-m core sample taken from Tatoosh intrusive rock using the whole-core cryogenic magnetometer, and deconvolved the data utilizing a low-pass-filter in frequency space. The filter shape and cut-off frequency of the low-pass-filter were determined subjectively by visual analysis.

Constable and Parker (1991) developed a deconvolution scheme using a smoothness-constrained least squares method and applied it to paleomagnetic data from a deep-sea sediment core. They assumed that the magnetizations changed smoothly and expressed the data, the magnetization and the sensor response in terms of cubic spline functions. The smoothness was measured by a 2-norm of the second derivative of the magnetization. The degree of smoothness was determined so that the fitting residual equals the observational error. The observational errors were estimated by looking at the rms value of measurements beyond the region of influence of the core magnetization.

In this paper, we present a new deconvolution scheme based on Bayesian statistics. The method is similar to that of Constable and Parker (1991), in that the deconvolution is also conducted as a smoothness-constrained least squares method with the smoothness measured by a

2-norm of the second derivative of the magnetizations. The difference between our method and that of Constable and Parker (1991) resides in the determination of smoothness. They determined the smoothness by estimating the noise level of the data, whereas we optimize the smoothness objectively by using *ABIC* (A Bayesian Information Criterion; Akaike, 1980) minimization. *ABIC* is a criterion based on Bayes' theorem to which we can introduce prior distribution without ambiguity. *ABIC* minimization have already been applied successfully to several geophysical data analyses (Murata, 1990; Tamura *et al.*, 1991).

The new deconvolution scheme was applied to whole-core remanence data from a 70-cm long "U-channel" sample measured by a whole-core cryogenic magnetometer. The magnetization calculated by the deconvolution was compared with the magnetization measured directly on the thin-sliced specimens taken from the U-channel. In addition, synthetic whole-core remanence data with different noise levels were produced, so the deconvolution could be tested with different S/N ratios.

## 2. Formulation of the Deconvolution Scheme

In our deconvolution model, measurement intervals are set to be uniform and we assume the following conditions: (1) magnetization is uniform within each unit slice (2) the deconvolution can be conducted separately in each axis. The second assumption means that the long-core samples are put in the center of the magnetometer, and three orthogonal vector components of the magnetization are picked up independently. The samples put on the off-centered position (i.e. ODP's routine measurements on archive half samples) produces cross terms between different axes; we will deal with this configuration in another paper.

Whole-core data measured by a cryogenic magnetometer is a linear function of magnetization of the sample described by the sensor response function as

$$\mathbf{d} = \mathbf{R}\mathbf{m} + \mathbf{e}, \quad (1)$$

$$\mathbf{d} = \begin{pmatrix} d_1 \\ d_2 \\ \vdots \\ d_N \end{pmatrix}, \quad \mathbf{m} = \begin{pmatrix} m_1 \\ m_2 \\ \vdots \\ m_M \end{pmatrix}, \quad \mathbf{R} = \begin{pmatrix} R_\ell & & 0 \\ \vdots & \ddots & \\ R_0 & & R_r \\ \vdots & \ddots & \vdots \\ R_{-r} & & R_0 \\ & \ddots & \vdots \\ 0 & & R_{-\ell} \end{pmatrix}, \quad \mathbf{e} = \begin{pmatrix} \varepsilon_1 \\ \varepsilon_2 \\ \vdots \\ \varepsilon_N \end{pmatrix}.$$

Here  $\mathbf{d}$  denotes the set of whole-core data,  $\mathbf{m}$  is the magnetization of the sample,  $\mathbf{R}$  is a matrix filled with columns of the sensor responses, and  $\mathbf{e}$  is the noise in the whole-core data.  $N$  is the total number of measured points, and  $M$  is the number of measured points within the sample.  $\ell$  is the number of measured points beyond the sample,  $r$  is half the number of sensor responses, and  $R_0$  corresponds to the center of the sensor response. The magnetization  $\mathbf{m}$  can be obtained by solving Eq. (1) according to the least-squares method which minimizes the summation

$$S = \|\mathbf{d} - \mathbf{R}\mathbf{m}\|^2. \quad (2)$$

This procedure exaggerates the high frequency component of the noise,  $\mathbf{e}$ . We assume that the magnetization changes smoothly and use a smoothness-stabilized least squares method to reduce the high frequency noise. The smoothness-stabilized least squares fit is calculated by minimizing the summation with second-order finite differences

$$S^* = \|\mathbf{d} - \mathbf{R}\mathbf{m}\|^2 + \lambda\|\mathbf{D}\mathbf{m}\|^2, \quad (3)$$

$$\mathbf{D} = \begin{pmatrix} \alpha & & & & \\ -\beta & \beta & & & 0 \\ 1 & -2 & 1 & & \\ & \ddots & \ddots & \ddots & \\ 0 & & & 1 & -2 & 1 \end{pmatrix},$$

where  $\mathbf{D}$  is a matrix representing second-order differences, and  $\alpha$  and  $\beta$  are properly chosen parameters. Thus  $\mathbf{Dm}$  represents second order difference of the magnetization.  $\lambda$  is introduced as a hyper parameter which controls smoothness of the magnetization  $\mathbf{m}$ ; and the smoothness of the magnetization increases as  $\lambda$  increases.

In order to decide the best estimates of  $\lambda$ , we applied the Bayes' theorem to the deconvolution. The smoothness-stabilized deconvolution can be understood in terms of a likelihood maximization process on a Bayes model. According to Bayes' theorem, the posterior distribution of the magnetization  $p(\mathbf{m}|\mathbf{d}, \nu, \tau)$  is constituted by the likelihood function and the prior distribution as

$$p(\mathbf{m}|\mathbf{d}, \nu, \tau) \propto L(\mathbf{d}|\mathbf{m}, \nu) \rho(\mathbf{m}|\tau). \quad (4)$$

Here  $L(\mathbf{d}|\mathbf{m}, \nu)$  is the likelihood of the whole-core data,  $\mathbf{d}$ , and  $\rho(\mathbf{m}|\tau)$  is the prior distribution of the magnetization,  $\mathbf{m}$ . Under an assumption that the error distribution is Gaussian with zero mean and variance  $\nu$ , the likelihood of the whole-core measured data  $\mathbf{d}$  is given explicitly as

$$L(\mathbf{d}|\mathbf{m}, \nu) = \left(\frac{1}{2\pi\nu}\right)^{\frac{N}{2}} \exp\left\{-\frac{1}{2\nu}\|\mathbf{d} - \mathbf{Rm}\|^2\right\}. \quad (5)$$

As we assume that the magnetization changes smoothly, the second order difference of the magnetization can be expressed by a Gaussian distribution with zero mean and variance  $\tau$ . The prior distribution of  $\mathbf{m}$  is given as

$$\rho(\mathbf{m}|\tau) = \left(\frac{1}{2\pi\tau}\right)^{\frac{M}{2}} \exp\left\{-\frac{1}{2\tau}\|\mathbf{Dm}\|^2\right\}. \quad (6)$$

By substituting Eq. (5) and Eq. (6) to Eq. (4), we get the final form of posterior distribution

$$p(\mathbf{d}|\mathbf{m}, \nu, u) = K \left(\frac{1}{2\pi\nu}\right)^{\frac{N}{2}} \left(\frac{u^2}{2\pi\nu}\right)^{\frac{M}{2}} \exp\left\{-\frac{1}{2\nu}\left[\|\mathbf{d} - \mathbf{Rm}\|^2 + u^2\|\mathbf{Dm}\|^2\right]\right\} d\mathbf{m}, \quad (7)$$

where  $K$  is a normalization constant. We introduced hyper parameter  $u^2 (= \nu/\tau)$  to express the degree of smoothness. It is easily understood by properly replacing  $u^2$  to  $\lambda$  that the formula in the bracket of Eq. (7) is identical to Eq. (3). This means that maximizing Eq. (7) in terms of  $\mathbf{m}$  is a constrained least squares problem. Once parameter  $u$  is given,  $\mathbf{m}$  of maximum likelihood can be obtained using the least squares method, namely minimizing the value of the formula in the bracket of Eq. (7).

The optimum value of the hyper parameter  $u$  can be determined objectively by minimizing a Bayesian Information Criterion (*ABIC*; Akaike, 1980), which is given as

$$ABIC = -2 \log(\text{maximum marginal likelihood}) + 2(\text{number of adjusted hyperparameters}). \quad (8)$$

Here, the maximum marginal likelihood function is given as

$$L_{\text{marginal}}(u, \nu) = \int L(\mathbf{d}|\mathbf{m}, \nu) \rho(\mathbf{m}|u) d\mathbf{m}. \quad (9)$$

$ABIC$  of our deconvolution model is calculated by substituting Eq. (5) and Eq. (6) into Eq. (9) and again into Eq. (8), to get

$$ABIC = N \log s^2 - M \log u^2 - \log |\mathbf{D}^t \mathbf{D}| + \log |\mathbf{R}^t \mathbf{R} + u^2 \mathbf{D}^t \mathbf{D}| + N - N \log N + N \log 2\pi + 2, \quad (10)$$

$$s^2 = \min_{\mathbf{m}} \{ \|\mathbf{d} - \mathbf{Rm}\|^2 + u^2 \|\mathbf{Dm}\|^2 \}.$$

Thus, the maximum likelihood solution, under an assumption of smoothly changing magnetization, can be obtained for the  $u$  value that minimizes  $ABIC$  given by Eq. (10).

### 3. Samples and Measurements

We used a 70-cm long "U-channel" sample taken from an advanced hydraulic piston core sample (124-768B-10H-2, 80–150 cm) from ODP Site 768, drilled in the southeast Sulu basin. A "U-channel" is a U-shaped sampling tool made of plastic (24 × 24 mm in cross section) designed for continuous sampling of ODP cores (Tauxe *et al.*, 1983). The core we used is homogeneous and mainly composed of foraminiferal and nannofossiliferous marl (Rangin *et al.*, 1990). The intensity of natural remanent magnetization of the sample is very high ranging from 10 to 100 mA/m. Magnetic minerals present are assumed to be Fe-rich titanomagnetite on the basis of thermomagnetic analysis (the Curie temperature is about 540°C). The sample had a rectangular 24 × 24 × 15 mm hole due to sampling for shipboard paleomagnetic study between 109 cm and 111.5 cm.

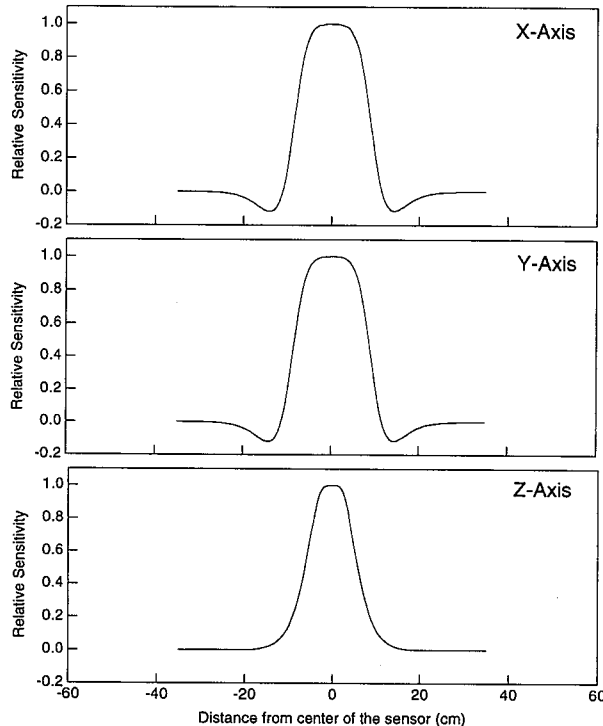


Fig. 1. Normalized sensor-response curves for the X, Y and Z axes of the cryogenic magnetometer (HOXAN SRM) at Doshisha University. The curves were determined by measuring a small cube of basalt.

NRM measurements were carried out at intervals of 5 mm using a whole-core cryogenic magnetometer (HOXAN SRM) at Doshisha University. We also measured beyond the region of the "U-channel" sample (25 cm on both sides along axis) to stabilize the solution. The Z axis is parallel to the long axis of the core sample, and X and Y axes are transverse. The noise levels of the magnetometer are  $5 \times 10^{-11} \text{ Am}^2$  in X and Y axes, and  $3 \times 10^{-11} \text{ Am}^2$  in Z axis (Ishige *et al.*, 1989). The "U-channel" sample was fixed on a practically non-magnetic polyvinyl chloride guide and inserted, together with the guide into the bore hole of the magnetometer step-by-step. The cryogenic magnetometer had three sets of pick up coils and the remanent magnetization vector was determined by a single measurements. The sensor response curves of three axes were measured at intervals of 5 mm with a small reference sample ( $5 \times 5 \times 5 \text{ mm}$  basalt cube) whose intensity is  $3.61 \times 10^{-6} \text{ Am}^2$  (Fig. 1). The response curve of the Z axis is different from those of the X and Y axes because the configuration of the sample and the "Z" pick up coil is different. One hundred and forty thin sections of 5-mm thick were cut from the same "U-channel" sample and put on pyrex glass plates. NRMs were measured using a normal cryogenic magnetometer (ScT C112) at Kyoto University. The magnetizations of thin sections were used for comparison with those of deconvolved magnetizations and also for synthesizing artificial data. The volume of the each section is not exactly the same because it is difficult to keep a constant thickness of 5 mm. The volume of each specimen was estimated by using the weight of each specimen in wet condition assuming constant density throughout the "U-channel" sample. The average density of the sample was calculated to be  $1.3 \text{ g/cm}^3$  from the total volume of the "U-channel" sample and the sum of weights. The volume of each specimen was calculated from the average density and the weight of each specimen. The magnetizations per unit volume were calculated using these volumes.

#### 4. Applications of the Deconvolution Scheme

##### 4.1 Synthesized data

Synthetic whole-core data with various noise-levels were generated, then deconvolved to investigate the characteristics of our deconvolution scheme. The synthesized data was produced by convolving the X-axis component of magnetizations of the thin sections with the sensor response function and superimposing zero mean Gaussian noise. The same Gaussian noise was used, with only the magnitude being changed in different cases, to avoid possible artifacts from different distributions. The original data were chosen so that the real frequency distribution could be simulated in the synthesized data.

Synthesized data with three different levels of noise (S/N ratios of 10, 100 and 1000) were deconvolved. Minimum *ABIC* values were searched by dividing the  $\ln u$  value half-by-half down to 0.25 intervals; *ABIC* values calculated for each S/N ratio were plotted versus  $\ln u$  (Fig. 2, solid circles). These diagrams show that the *ABIC* values reach a minimum when  $\ln u$  equals to  $-1.25$ ,  $-3.5$  and  $-6.25$  for S/N ratios of 10, 100, and 1000, respectively (Table 1). The  $u$  value

Table 1. Statistical parameters at minimum *ABIC* for the results of deconvolution on synthesized data with S/N ratios of 10, 100 and 1000.

S/N ratio	noise level ( $\text{Am}^2$ )	minimum	$\ln u$	rms of residuals of	rms of residuals of
		<i>ABIC</i>		total moment from the moment of model ( $\text{Am}^2$ )	deconvolved magnetization from original (mA/m)
10	$9.1 \times 10^{-5}$	-3662	-1.25	$8.5 \times 10^{-5}$	11.9
100	$9.1 \times 10^{-6}$	-4664	-3.5	$8.5 \times 10^{-6}$	9.3
1000	$9.1 \times 10^{-7}$	-5575	-6.25	$8.5 \times 10^{-7}$	7.7

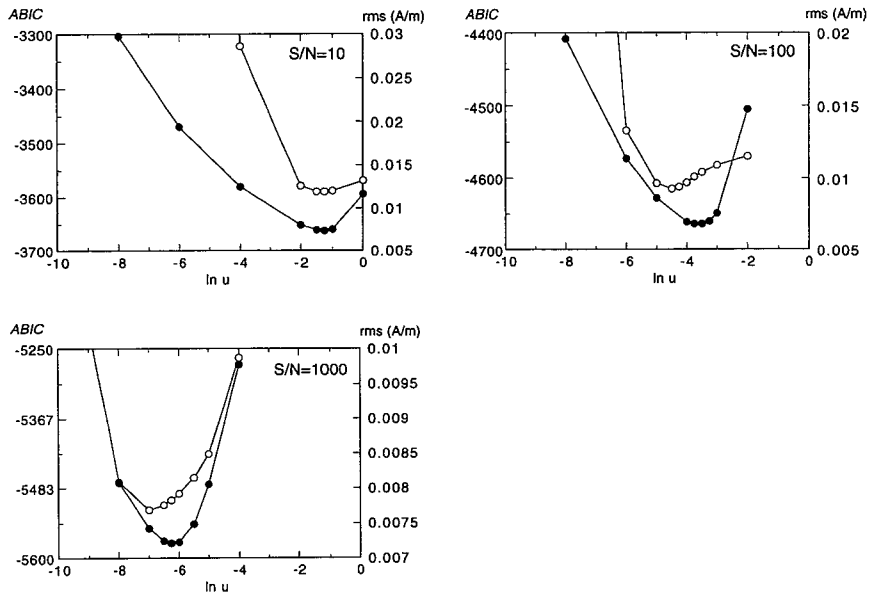


Fig. 2.  $ABIC$  values (solid circles) plotted for  $S/N$  ratios of 10, 100 and 1000. Root mean square ( $rms$ ) differences between magnetization after deconvolution and the original whole-core magnetization are displayed by open circles.

for minimum  $ABIC$  shifts to a lower value with decreasing noise levels, whence a shorter wave length structure is obtained. Root mean square values of the differences between the deconvolved magnetization and original magnetization are also plotted in Fig. 2 (open circles). These values come to minimum at slightly smaller  $u$  values than the  $u$  values that minimize  $ABIC$ . The magnetizations deconvolved from the synthesized data for each  $S/N$  ratios are plotted in Fig. 3 together with the original magnetization of thin sections. Misfit between the original magnetization and deconvolved magnetization is substantially reduced as the noise level decreases. The large fluctuations around 40–45 cm are not resolved by the deconvolved record. The residuals of original (synthetic) whole-core data versus whole-core data convolved from deconvolved magnetization were found to have a white noise distribution, which is consistent with the characteristics of the noise superimposed before deconvolution. The root mean squares ( $rms$ ) of the residuals of the  $ABIC$  minimizing deconvolution agree very well with the noise levels superimposed on the synthesized data (Table 1).

#### 4.2 Real data

The three vector components of magnetization measured on the “U-channel” sample were deconvolved separately by  $ABIC$  minimization. In Fig. 4,  $ABIC$  values are plotted versus  $\ln u$  for each axis. The  $ABIC$  values lie on downward-convex curves and come to minima at the  $\ln u$  values of  $-3.00$ ,  $-4.00$  and  $-4.50$  for the X, Y and Z axis, respectively. Figures 5, 6 and 7 show the results of deconvolution at minimum  $ABIC$  values for the X, Y, and Z components of magnetization, respectively. These figures show (a) magnetization after deconvolution of whole-core data (solid line) and magnetization of thin sections (dots), (b) output of whole-core measurements (solid line) and convolution of thin sections (dots), (c) residuals, and (d) sensor response functions. The magnetization obtained by deconvolution on whole-core data agrees well with the magnetization of the thin sections in X, Y, and Z axes.

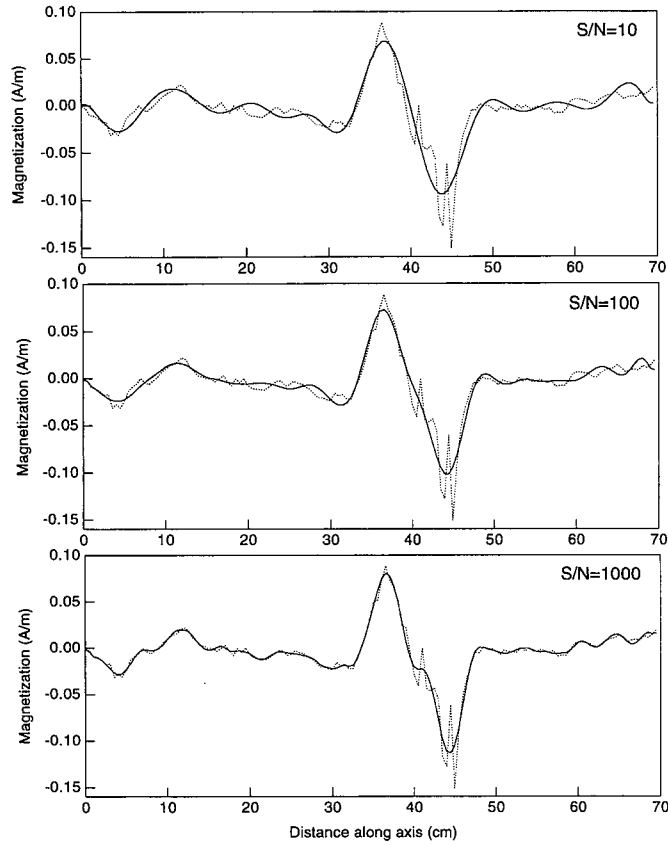


Fig. 3. Magnetization deconvolved from the artificial data for S/N ratios of 10, 100 and 1000 (solid lines) compared with the original magnetization of thin sections (broken lines).

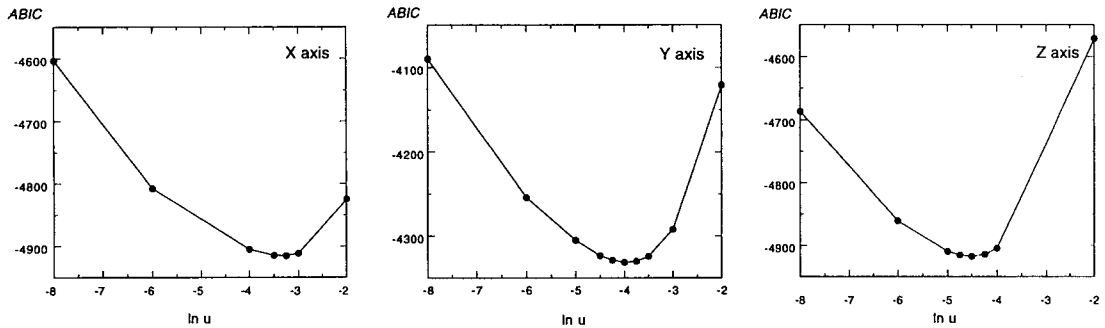


Fig. 4. ABIC plotted against natural log of  $u$  for X, Y and Z components of magnetizations of the "U-channel" sample.

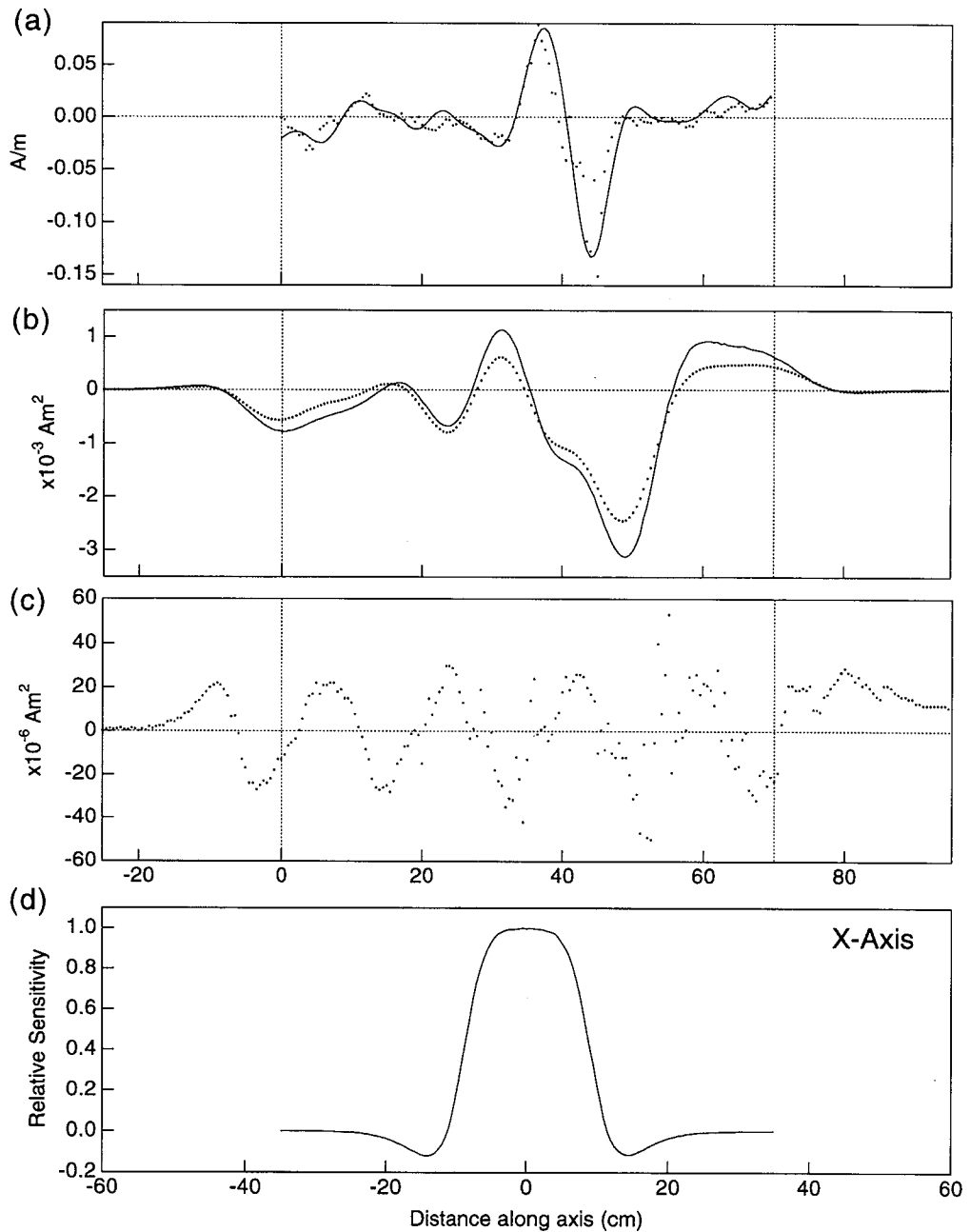


Fig. 5. Deconvolution of the X-component of magnetization for the "U-channel" sample taken from 124-768B-10H-2, 80–150 cm (ODP core sample). The vertical broken lines correspond to the ends of the sample. (a) Magnetization after deconvolution of whole-core data (solid line) and magnetization measured directly on thin sections (dots). (b) Pass-through measurement data (solid line) and convolution of NRMs of thin sections (dots). (c) Plot of residuals calculated by subtracting original magnetic moment from convolution of magnetization after deconvolution. (d) Normalized sensor response curve for X-axis. All the data points were measured at intervals of 5 mm.



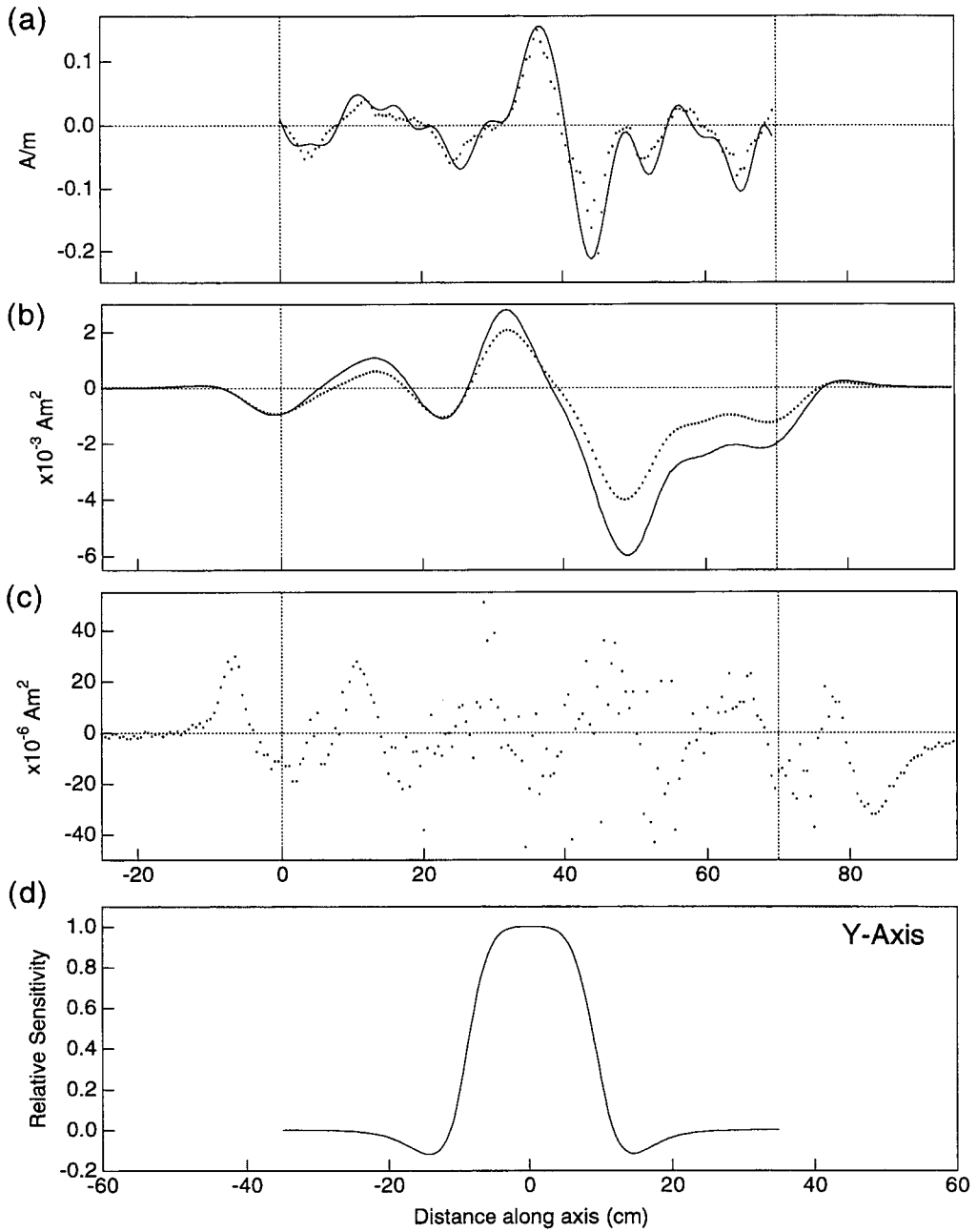


Fig. 6. As per Fig. 5, for the Y-component of magnetization.

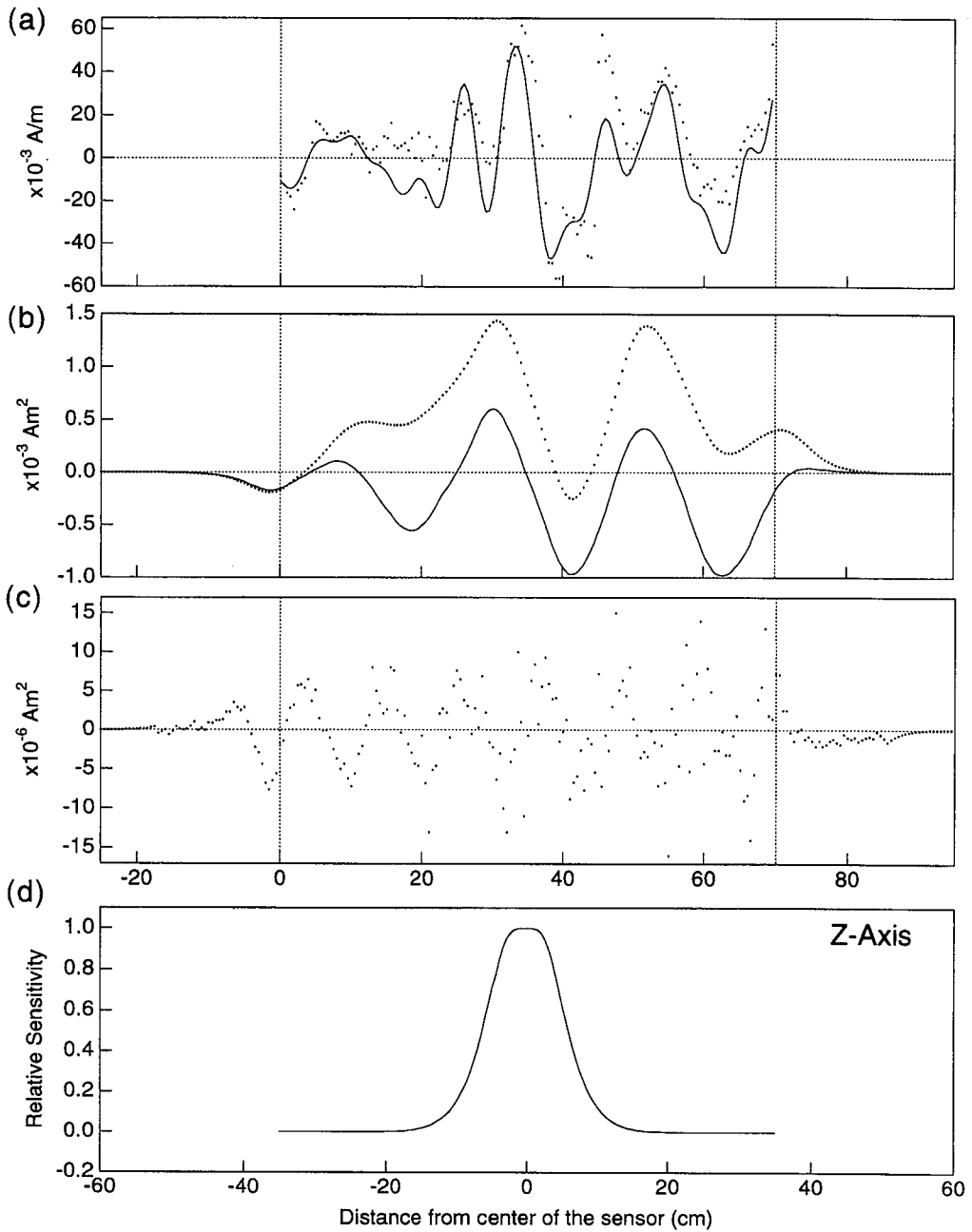


Fig. 7. As per Fig. 5, for the Z-component of magnetization.

## 5. Discussion

### 5.1 Synthesized data

The results of deconvolution on the synthesized data showed that our deconvolution scheme by *ABIC* minimization works very well. In Fig. 2, the value of  $u$  where *ABIC* comes to minimum is slightly larger than the value of  $u$  that minimizes the rms of residuals (deconvolved magnetization minus original magnetization). This may come from the large fluctuations around 40–45 cm and the frequency distribution of the original magnetization data.

The synthesized data with S/N ratio of 100 was deconvolved using the program by Constable and Parker (1991) for comparison. Noise level estimation is needed for their program to determine the fitting tolerance (smoothness). The changes of rms difference between deconvolved signal and directly measured magnetization for different estimated noise levels are listed in Table 2. The results show that the rms comes to a minimum when the estimated noise level is chosen as  $1.5 \times 10^{-5} \text{ Am}^2$ . The results for estimated noise levels of  $9.1 \times 10^{-6} \text{ Am}^2$  and  $1.5 \times 10^{-5} \text{ Am}^2$  are shown in Fig. 8 (open circles) with our result for minimum *ABIC* (solid lines) and directly measured magnetization (broken lines). The noise level of  $9.1 \times 10^{-6} \text{ Am}^2$  corresponds to the S/N ratio of 100 for this synthesized data. The deconvolved signal is disturbed by high frequency noise and is far from the original magnetization. The results may be slightly affected by the difference between our method of convolution of the magnetization and C&P's method in terms of cubic spline. The magnetization after deconvolution for the noise level of  $1.5 \times 10^{-5} \text{ Am}^2$ , which is not so far from  $9.1 \times 10^{-6} \text{ Am}^2$ , were not disturbed by high frequency noise and are similar to the *ABIC* deconvolution result and the original magnetization. The difference of the solutions near the noise level of  $1.0 \times 10^{-5} \text{ Am}^2$  is critical and it can be said that careful noise estimation is indispensable for C&P's program.

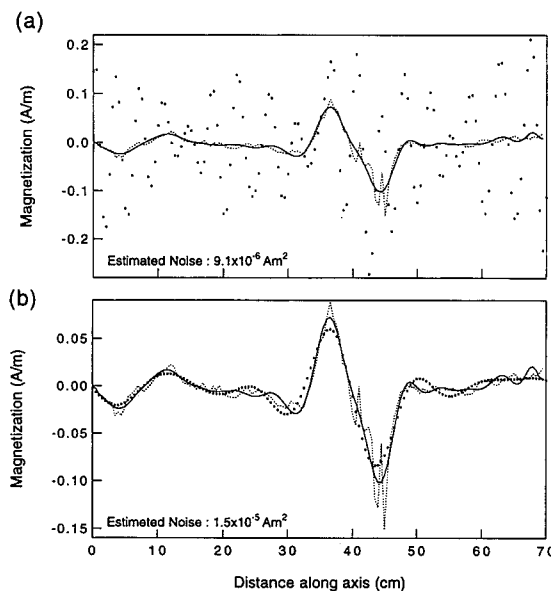


Fig. 8. Synthesized data with S/N ratio of 100 deconvolved using the program by Constable and Parker (1991). The magnetizations for estimated noise levels of (a)  $9.1 \times 10^{-6} \text{ Am}^2$  and (b)  $1.5 \times 10^{-5} \text{ Am}^2$  (solid circles) are shown with the magnetization of *ABIC* deconvolution (solid lines) and the magnetization of thin sections (broken lines).

2-norm of the second derivative of the magnetizations. The difference between our method and that of Constable and Parker (1991) resides in the determination of smoothness. They determined the smoothness by estimating the noise level of the data, whereas we optimize the smoothness objectively by using *ABIC* (A Bayesian Information Criterion; Akaike, 1980) minimization. *ABIC* is a criterion based on Bayes' theorem to which we can introduce prior distribution without ambiguity. *ABIC* minimization have already been applied successfully to several geophysical data analyses (Murata, 1990; Tamura *et al.*, 1991).

The new deconvolution scheme was applied to whole-core remanence data from a 70-cm long "U-channel" sample measured by a whole-core cryogenic magnetometer. The magnetization calculated by the deconvolution was compared with the magnetization measured directly on the thin-sliced specimens taken from the U-channel. In addition, synthetic whole-core remanence data with different noise levels were produced, so the deconvolution could be tested with different S/N ratios.

## 2. Formulation of the Deconvolution Scheme

In our deconvolution model, measurement intervals are set to be uniform and we assume the following conditions: (1) magnetization is uniform within each unit slice (2) the deconvolution can be conducted separately in each axis. The second assumption means that the long-core samples are put in the center of the magnetometer, and three orthogonal vector components of the magnetization are picked up independently. The samples put on the off-centered position (i.e. ODP's routine measurements on archive half samples) produces cross terms between different axes; we will deal with this configuration in another paper.

Whole-core data measured by a cryogenic magnetometer is a linear function of magnetization of the sample described by the sensor response function as

$$\mathbf{d} = \mathbf{R}\mathbf{m} + \mathbf{e}, \quad (1)$$

$$\mathbf{d} = \begin{pmatrix} d_1 \\ d_2 \\ \vdots \\ d_N \end{pmatrix}, \quad \mathbf{m} = \begin{pmatrix} m_1 \\ m_2 \\ \vdots \\ m_M \end{pmatrix}, \quad \mathbf{R} = \begin{pmatrix} R_\ell & & 0 \\ \vdots & \ddots & \\ R_0 & & R_r \\ \vdots & \ddots & \vdots \\ R_{-r} & & R_0 \\ & \ddots & \vdots \\ 0 & & R_{-\ell} \end{pmatrix}, \quad \mathbf{e} = \begin{pmatrix} \varepsilon_1 \\ \varepsilon_2 \\ \vdots \\ \varepsilon_N \end{pmatrix}.$$

Here  $\mathbf{d}$  denotes the set of whole-core data,  $\mathbf{m}$  is the magnetization of the sample,  $\mathbf{R}$  is a matrix filled with columns of the sensor responses, and  $\mathbf{e}$  is the noise in the whole-core data.  $N$  is the total number of measured points, and  $M$  is the number of measured points within the sample.  $\ell$  is the number of measured points beyond the sample,  $r$  is half the number of sensor responses, and  $R_0$  corresponds to the center of the sensor response. The magnetization  $\mathbf{m}$  can be obtained by solving Eq. (1) according to the least-squares method which minimizes the summation

$$S = \|\mathbf{d} - \mathbf{R}\mathbf{m}\|^2. \quad (2)$$

This procedure exaggerates the high frequency component of the noise,  $\mathbf{e}$ . We assume that the magnetization changes smoothly and use a smoothness-stabilized least squares method to reduce the high frequency noise. The smoothness-stabilized least squares fit is calculated by minimizing the summation with second-order finite differences

$$S^* = \|\mathbf{d} - \mathbf{R}\mathbf{m}\|^2 + \lambda\|\mathbf{D}\mathbf{m}\|^2, \quad (3)$$

$$\mathbf{D} = \begin{pmatrix} \alpha & & & & \\ -\beta & \beta & & & 0 \\ 1 & -2 & 1 & & \\ & \ddots & \ddots & \ddots & \\ 0 & & & 1 & -2 & 1 \end{pmatrix},$$

where  $\mathbf{D}$  is a matrix representing second-order differences, and  $\alpha$  and  $\beta$  are properly chosen parameters. Thus  $\mathbf{D}\mathbf{m}$  represents second order difference of the magnetization.  $\lambda$  is introduced as a hyper parameter which controls smoothness of the magnetization  $\mathbf{m}$ ; and the smoothness of the magnetization increases as  $\lambda$  increases.

In order to decide the best estimates of  $\lambda$ , we applied the Bayes' theorem to the deconvolution. The smoothness-stabilized deconvolution can be understood in terms of a likelihood maximization process on a Bayes model. According to Bayes' theorem, the posterior distribution of the magnetization  $p(\mathbf{m}|\mathbf{d}, \nu, \tau)$  is constituted by the likelihood function and the prior distribution as

$$p(\mathbf{m}|\mathbf{d}, \nu, \tau) \propto L(\mathbf{d}|\mathbf{m}, \nu) \rho(\mathbf{m}|\tau). \quad (4)$$

Here  $L(\mathbf{d}|\mathbf{m}, \nu)$  is the likelihood of the whole-core data,  $\mathbf{d}$ , and  $\rho(\mathbf{m}|\tau)$  is the prior distribution of the magnetization,  $\mathbf{m}$ . Under an assumption that the error distribution is Gaussian with zero mean and variance  $\nu$ , the likelihood of the whole-core measured data  $\mathbf{d}$  is given explicitly as

$$L(\mathbf{d}|\mathbf{m}, \nu) = \left(\frac{1}{2\pi\nu}\right)^{\frac{N}{2}} \exp\left\{-\frac{1}{2\nu}\|\mathbf{d} - \mathbf{R}\mathbf{m}\|^2\right\}. \quad (5)$$

As we assume that the magnetization changes smoothly, the second order difference of the magnetization can be expressed by a Gaussian distribution with zero mean and variance  $\tau$ . The prior distribution of  $\mathbf{m}$  is given as

$$\rho(\mathbf{m}|\tau) = \left(\frac{1}{2\pi\tau}\right)^{\frac{M}{2}} \exp\left\{-\frac{1}{2\tau}\|\mathbf{D}\mathbf{m}\|^2\right\}. \quad (6)$$

By substituting Eq. (5) and Eq. (6) to Eq. (4), we get the final form of posterior distribution

$$p(\mathbf{d}|\mathbf{m}, \nu, u) = K \left(\frac{1}{2\pi\nu}\right)^{\frac{N}{2}} \left(\frac{u^2}{2\pi\nu}\right)^{\frac{M}{2}} \exp\left\{-\frac{1}{2\nu}\left[\|\mathbf{d} - \mathbf{R}\mathbf{m}\|^2 + u^2\|\mathbf{D}\mathbf{m}\|^2\right]\right\} d\mathbf{m}, \quad (7)$$

where  $K$  is a normalization constant. We introduced hyper parameter  $u^2 (= \nu/\tau)$  to express the degree of smoothness. It is easily understood by properly replacing  $u^2$  to  $\lambda$  that the formula in the bracket of Eq. (7) is identical to Eq. (3). This means that maximizing Eq. (7) in terms of  $\mathbf{m}$  is a constrained least squares problem. Once parameter  $u$  is given,  $\mathbf{m}$  of maximum likelihood can be obtained using the least squares method, namely minimizing the value of the formula in the bracket of Eq. (7).

The optimum value of the hyper parameter  $u$  can be determined objectively by minimizing a Bayesian Information Criterion (*ABIC*; Akaike, 1980), which is given as

$$ABIC = -2 \log(\text{maximum marginal likelihood}) + 2(\text{number of adjusted hyperparameters}). \quad (8)$$

Here, the maximum marginal likelihood function is given as

$$L_{\text{marginal}}(u, \nu) = \int L(\mathbf{d}|\mathbf{m}, \nu) \rho(\mathbf{m}|u) d\mathbf{m}. \quad (9)$$

$ABIC$  of our deconvolution model is calculated by substituting Eq. (5) and Eq. (6) into Eq. (9) and again into Eq. (8), to get

$$ABIC = N \log s^2 - M \log u^2 - \log |\mathbf{D}^t \mathbf{D}| + \log |\mathbf{R}^t \mathbf{R} + u^2 \mathbf{D}^t \mathbf{D}| + N - N \log N + N \log 2\pi + 2, \quad (10)$$

$$s^2 = \min_{\mathbf{m}} \{ \|\mathbf{d} - \mathbf{Rm}\|^2 + u^2 \|\mathbf{Dm}\|^2 \}.$$

Thus, the maximum likelihood solution, under an assumption of smoothly changing magnetization, can be obtained for the  $u$  value that minimizes  $ABIC$  given by Eq. (10).

### 3. Samples and Measurements

We used a 70-cm long "U-channel" sample taken from an advanced hydraulic piston core sample (124-768B-10H-2, 80–150 cm) from ODP Site 768, drilled in the southeast Sulu basin. A "U-channel" is a U-shaped sampling tool made of plastic (24 × 24 mm in cross section) designed for continuous sampling of ODP cores (Tauxe *et al.*, 1983). The core we used is homogeneous and mainly composed of foraminiferal and nannofossiliferous marl (Rangin *et al.*, 1990). The intensity of natural remanent magnetization of the sample is very high ranging from 10 to 100 mA/m. Magnetic minerals present are assumed to be Fe-rich titanomagnetite on the basis of thermomagnetic analysis (the Curie temperature is about 540°C). The sample had a rectangular 24 × 24 × 15 mm hole due to sampling for shipboard paleomagnetic study between 109 cm and 111.5 cm.

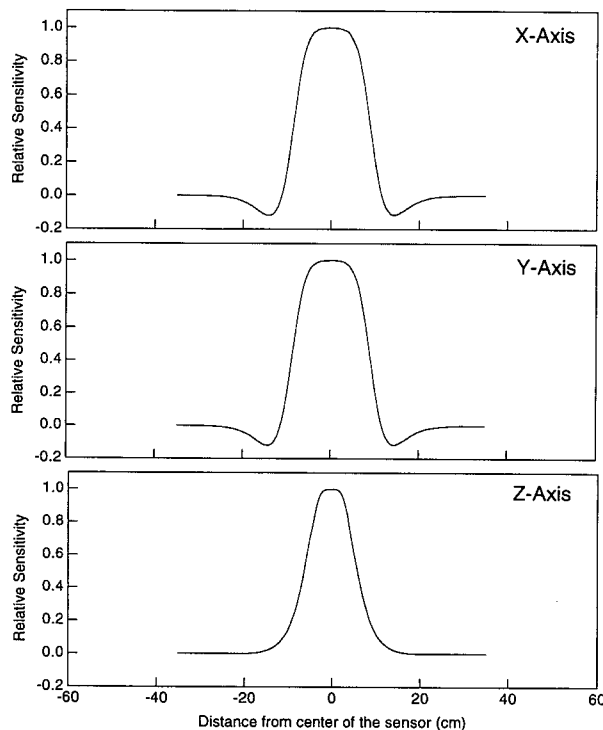


Fig. 1. Normalized sensor-response curves for the X, Y and Z axes of the cryogenic magnetometer (HOXAN SRM) at Doshisha University. The curves were determined by measuring a small cube of basalt.

NRM measurements were carried out at intervals of 5 mm using a whole-core cryogenic magnetometer (HOXAN SRM) at Doshisha University. We also measured beyond the region of the "U-channel" sample (25 cm on both sides along axis) to stabilize the solution. The Z axis is parallel to the long axis of the core sample, and X and Y axes are transverse. The noise levels of the magnetometer are  $5 \times 10^{-11} \text{ Am}^2$  in X and Y axes, and  $3 \times 10^{-11} \text{ Am}^2$  in Z axis (Ishige *et al.*, 1989). The "U-channel" sample was fixed on a practically non-magnetic polyvinyl chloride guide and inserted, together with the guide into the bore hole of the magnetometer step-by-step. The cryogenic magnetometer had three sets of pick up coils and the remanent magnetization vector was determined by a single measurements. The sensor response curves of three axes were measured at intervals of 5 mm with a small reference sample ( $5 \times 5 \times 5 \text{ mm}$  basalt cube) whose intensity is  $3.61 \times 10^{-6} \text{ Am}^2$  (Fig. 1). The response curve of the Z axis is different from those of the X and Y axes because the configuration of the sample and the "Z" pick up coil is different. One hundred and forty thin sections of 5-mm thick were cut from the same "U-channel" sample and put on pyrex glass plates. NRMs were measured using a normal cryogenic magnetometer (ScT C112) at Kyoto University. The magnetizations of thin sections were used for comparison with those of deconvolved magnetizations and also for synthesizing artificial data. The volume of the each section is not exactly the same because it is difficult to keep a constant thickness of 5 mm. The volume of each specimen was estimated by using the weight of each specimen in wet condition assuming constant density throughout the "U-channel" sample. The average density of the sample was calculated to be  $1.3 \text{ g/cm}^3$  from the total volume of the "U-channel" sample and the sum of weights. The volume of each specimen was calculated from the average density and the weight of each specimen. The magnetizations per unit volume were calculated using these volumes.

#### 4. Applications of the Deconvolution Scheme

##### 4.1 Synthesized data

Synthetic whole-core data with various noise-levels were generated, then deconvolved to investigate the characteristics of our deconvolution scheme. The synthesized data was produced by convolving the X-axis component of magnetizations of the thin sections with the sensor response function and superimposing zero mean Gaussian noise. The same Gaussian noise was used, with only the magnitude being changed in different cases, to avoid possible artifacts from different distributions. The original data were chosen so that the real frequency distribution could be simulated in the synthesized data.

Synthesized data with three different levels of noise (S/N ratios of 10, 100 and 1000) were deconvolved. Minimum *ABIC* values were searched by dividing the  $\ln u$  value half-by-half down to 0.25 intervals; *ABIC* values calculated for each S/N ratio were plotted versus  $\ln u$  (Fig. 2, solid circles). These diagrams show that the *ABIC* values reach a minimum when  $\ln u$  equals to  $-1.25$ ,  $-3.5$  and  $-6.25$  for S/N ratios of 10, 100, and 1000, respectively (Table 1). The  $u$  value

Table 1. Statistical parameters at minimum *ABIC* for the results of deconvolution on synthesized data with S/N ratios of 10, 100 and 1000.

S/N ratio	noise level ( $\text{Am}^2$ )	minimum		rms of residuals of	
		<i>ABIC</i>	$\ln u$	total moment from the moment of model ( $\text{Am}^2$ )	deconvolved magnetization from original (mA/m)
10	$9.1 \times 10^{-5}$	-3662	-1.25	$8.5 \times 10^{-5}$	11.9
100	$9.1 \times 10^{-6}$	-4664	-3.5	$8.5 \times 10^{-6}$	9.3
1000	$9.1 \times 10^{-7}$	-5575	-6.25	$8.5 \times 10^{-7}$	7.7

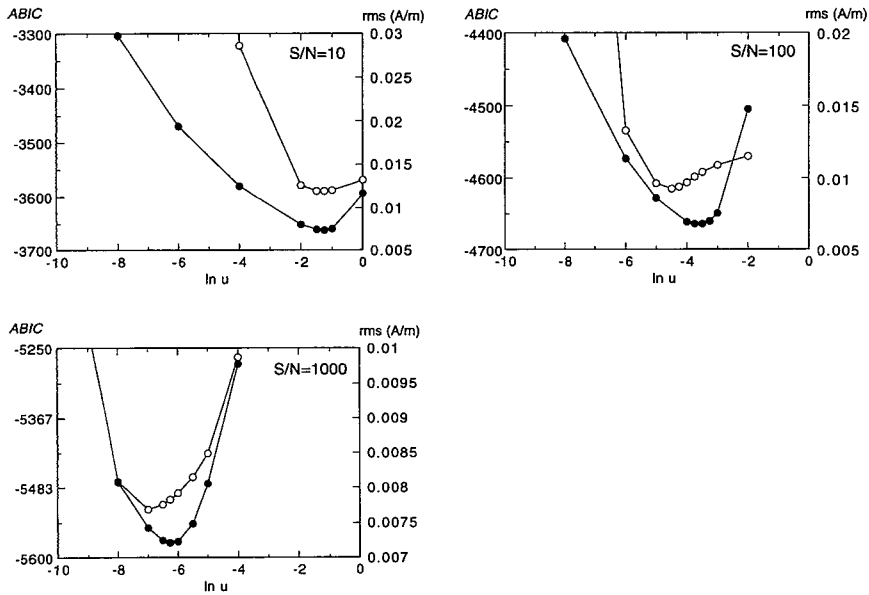


Fig. 2.  $ABIC$  values (solid circles) plotted for  $S/N$  ratios of 10, 100 and 1000. Root mean square (rms) differences between magnetization after deconvolution and the original whole-core magnetization are displayed by open circles.

for minimum  $ABIC$  shifts to a lower value with decreasing noise levels, whence a shorter wave length structure is obtained. Root mean square values of the differences between the deconvolved magnetization and original magnetization are also plotted in Fig. 2 (open circles). These values come to minimum at slightly smaller  $u$  values than the  $u$  values that minimize  $ABIC$ . The magnetizations deconvolved from the synthesized data for each  $S/N$  ratios are plotted in Fig. 3 together with the original magnetization of thin sections. Misfit between the original magnetization and deconvolved magnetization is substantially reduced as the noise level decreases. The large fluctuations around 40–45 cm are not resolved by the deconvolved record. The residuals of original (synthetic) whole-core data versus whole-core data convolved from deconvolved magnetization were found to have a white noise distribution, which is consistent with the characteristics of the noise superimposed before deconvolution. The root mean squares (rms) of the residuals of the  $ABIC$  minimizing deconvolution agree very well with the noise levels superimposed on the synthesized data (Table 1).

#### 4.2 Real data

The three vector components of magnetization measured on the “U-channel” sample were deconvolved separately by  $ABIC$  minimization. In Fig. 4,  $ABIC$  values are plotted versus  $\ln u$  for each axis. The  $ABIC$  values lie on downward-convex curves and come to minima at the  $\ln u$  values of  $-3.00$ ,  $-4.00$  and  $-4.50$  for the X, Y and Z axis, respectively. Figures 5, 6 and 7 show the results of deconvolution at minimum  $ABIC$  values for the X, Y, and Z components of magnetization, respectively. These figures show (a) magnetization after deconvolution of whole-core data (solid line) and magnetization of thin sections (dots), (b) output of whole-core measurements (solid line) and convolution of thin sections (dots), (c) residuals, and (d) sensor response functions. The magnetization obtained by deconvolution on whole-core data agrees well with the magnetization of the thin sections in X, Y, and Z axes.



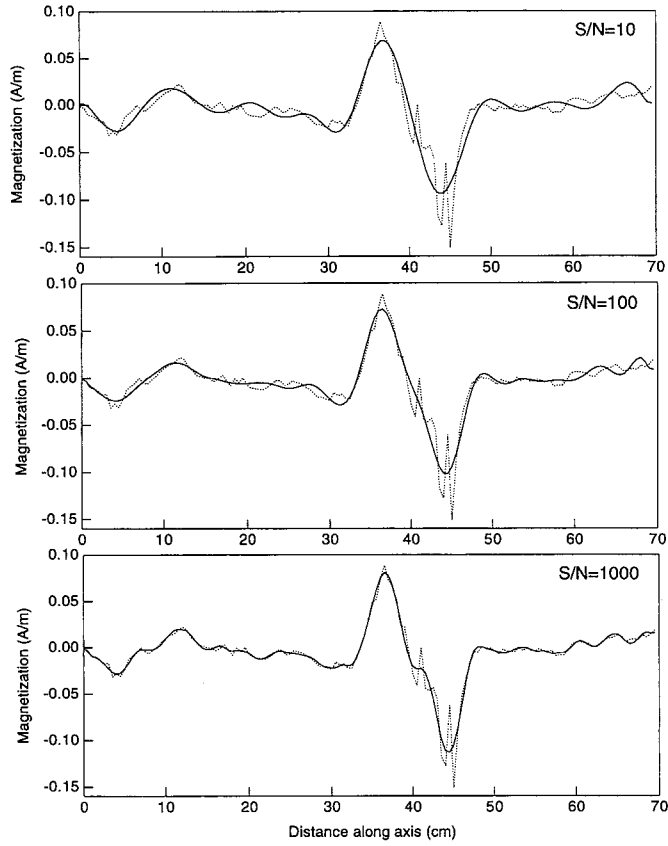


Fig. 3. Magnetization deconvolved from the artificial data for S/N ratios of 10, 100 and 1000 (solid lines) compared with the original magnetization of thin sections (broken lines).

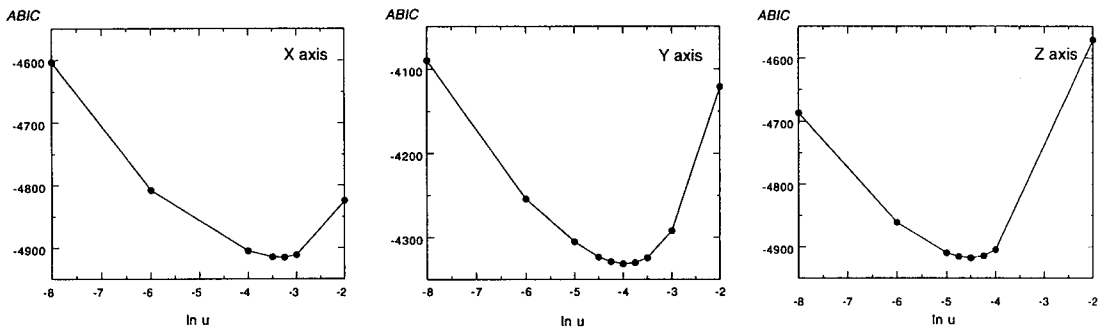


Fig. 4. ABIC plotted against natural log of  $u$  for X, Y and Z components of magnetizations of the "U-channel" sample.

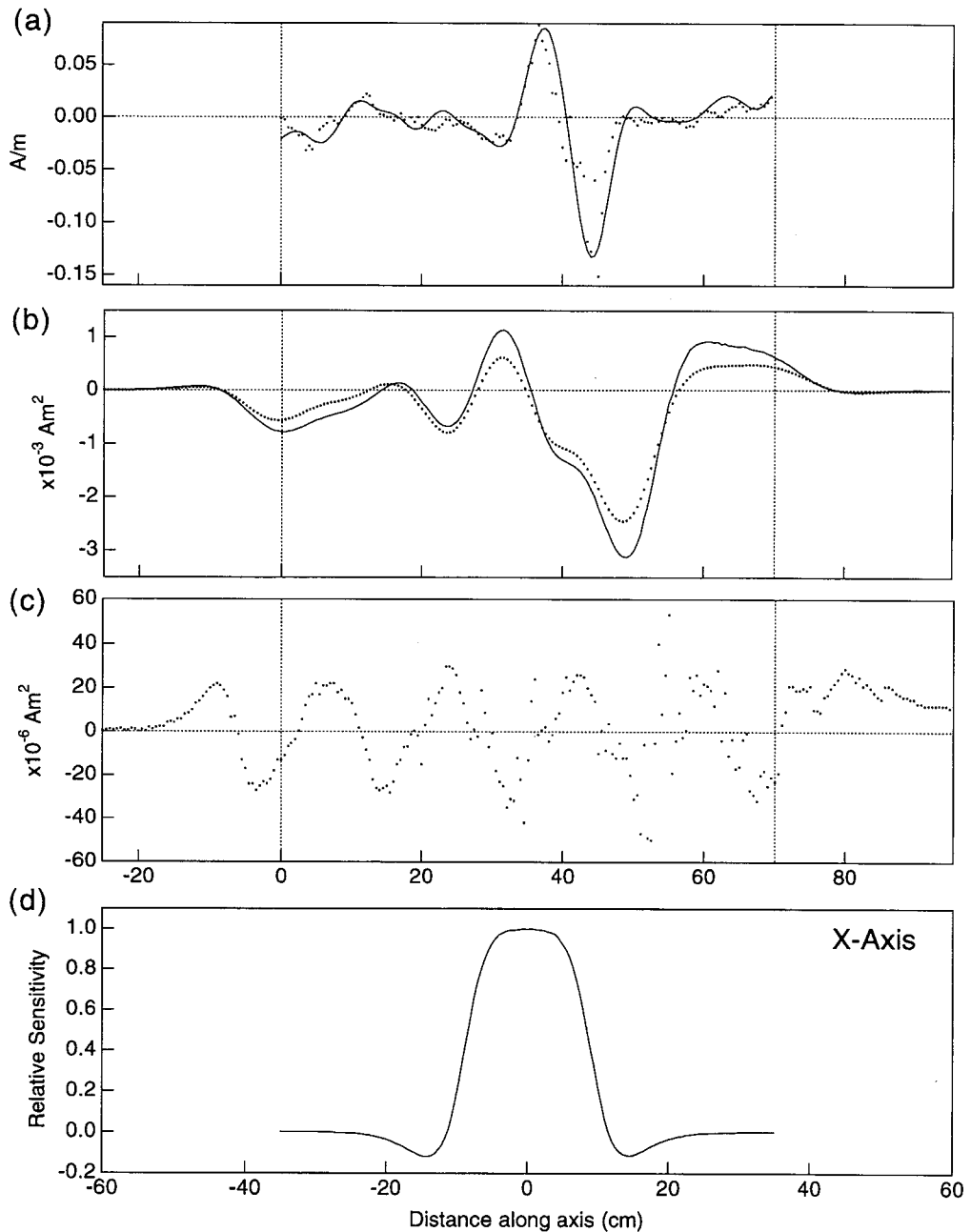


Fig. 5. Deconvolution of the X-component of magnetization for the "U-channel" sample taken from 124-768B-10H-2, 80–150 cm (ODP core sample). The vertical broken lines correspond to the ends of the sample. (a) Magnetization after deconvolution of whole-core data (solid line) and magnetization measured directly on thin sections (dots). (b) Pass-through measurement data (solid line) and convolution of NRMs of thin sections (dots). (c) Plot of residuals calculated by subtracting original magnetic moment from convolution of magnetization after deconvolution. (d) Normalized sensor response curve for X-axis. All the data points were measured at intervals of 5 mm.

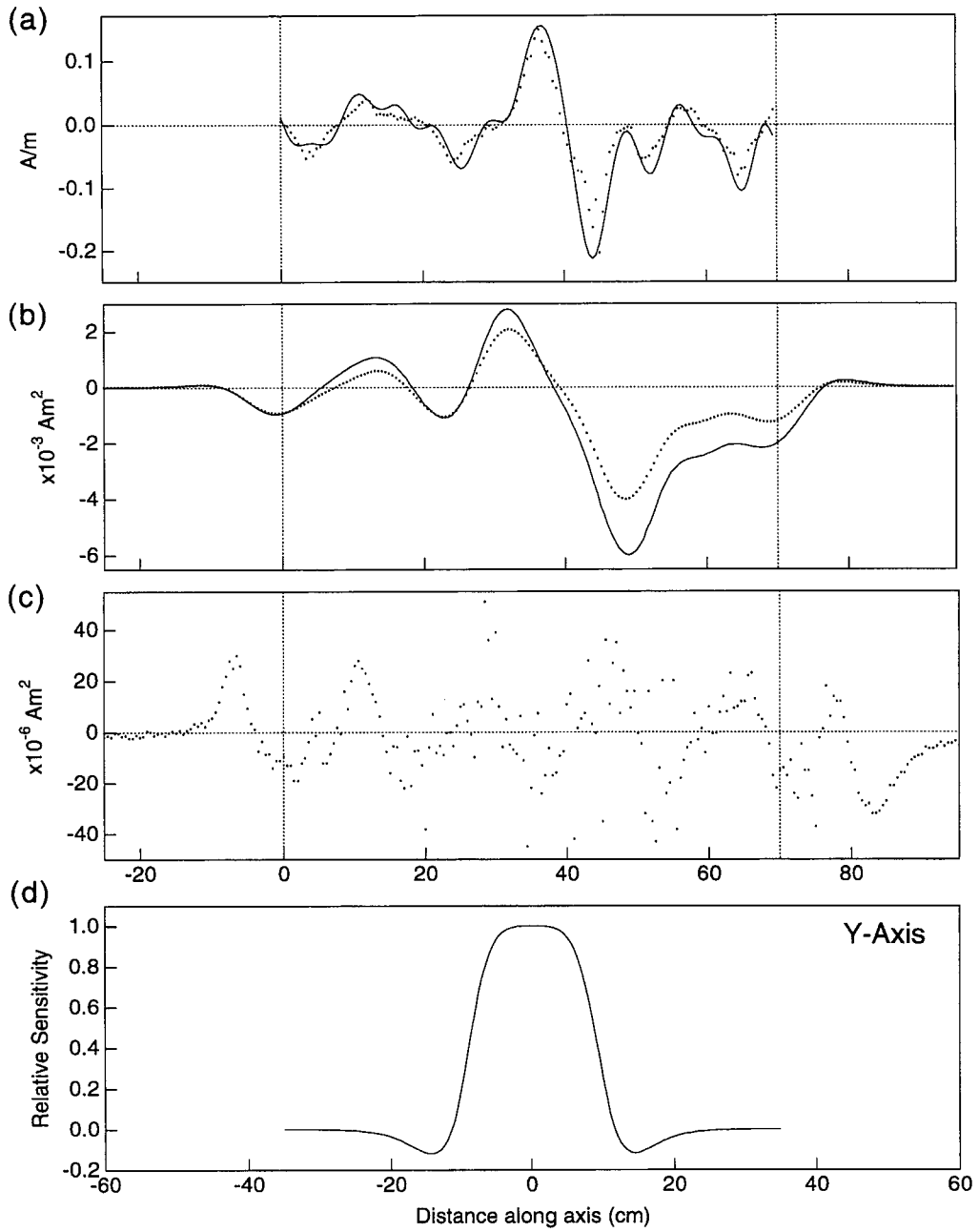


Fig. 6. As per Fig. 5, for the Y-component of magnetization.

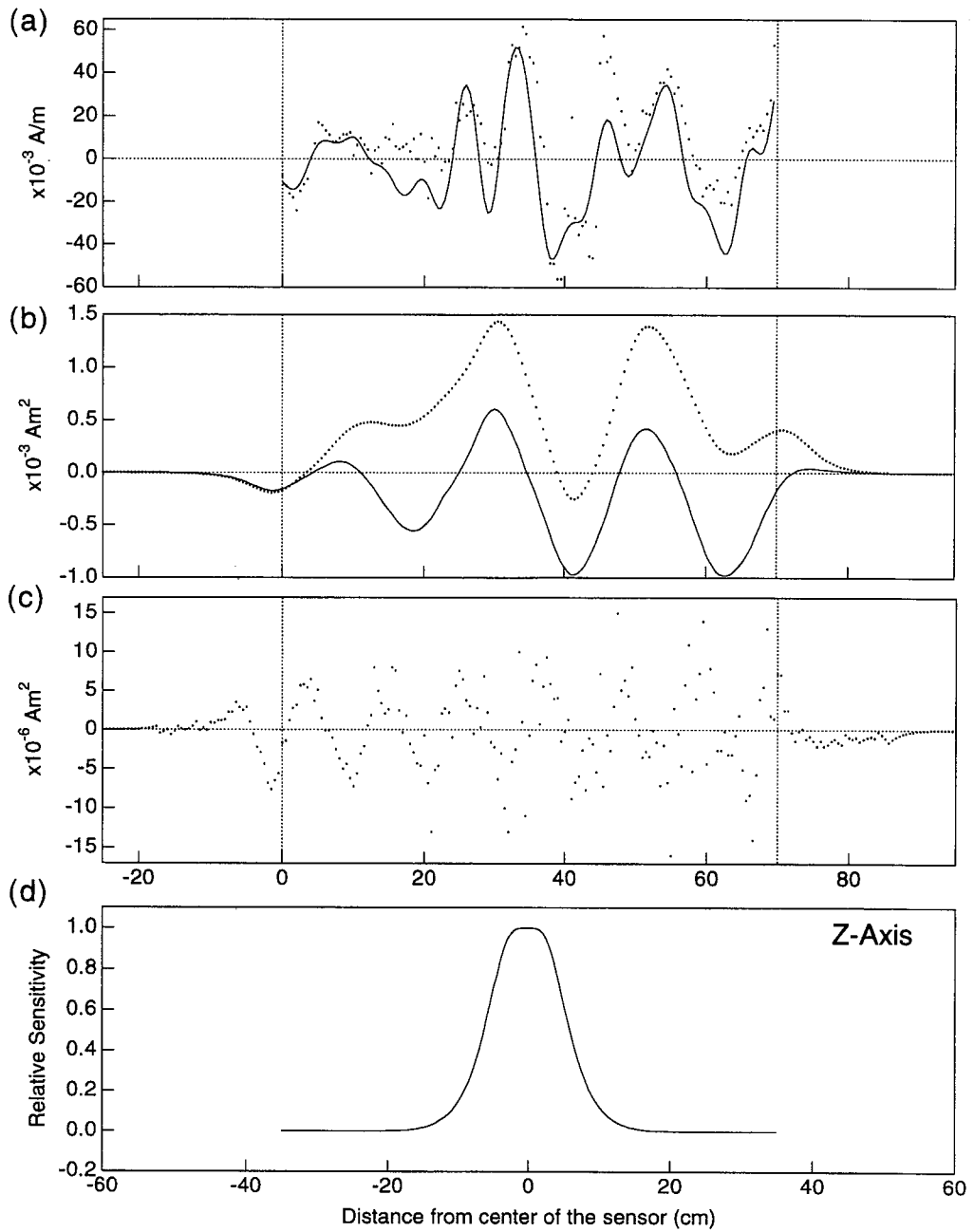


Fig. 7. As per Fig. 5, for the Z-component of magnetization.

## 5. Discussion

### 5.1 Synthesized data

The results of deconvolution on the synthesized data showed that our deconvolution scheme by *ABIC* minimization works very well. In Fig. 2, the value of  $u$  where *ABIC* comes to minimum is slightly larger than the value of  $u$  that minimizes the rms of residuals (deconvolved magnetization minus original magnetization). This may come from the large fluctuations around 40–45 cm and the frequency distribution of the original magnetization data.

The synthesized data with S/N ratio of 100 was deconvolved using the program by Constable and Parker (1991) for comparison. Noise level estimation is needed for their program to determine the fitting tolerance (smoothness). The changes of rms difference between deconvolved signal and directly measured magnetization for different estimated noise levels are listed in Table 2. The results show that the rms comes to a minimum when the estimated noise level is chosen as  $1.5 \times 10^{-5} \text{ Am}^2$ . The results for estimated noise levels of  $9.1 \times 10^{-6} \text{ Am}^2$  and  $1.5 \times 10^{-5} \text{ Am}^2$  are shown in Fig. 8 (open circles) with our result for minimum *ABIC* (solid lines) and directly measured magnetization (broken lines). The noise level of  $9.1 \times 10^{-6} \text{ Am}^2$  corresponds to the S/N ratio of 100 for this synthesized data. The deconvolved signal is disturbed by high frequency noise and is far from the original magnetization. The results may be slightly affected by the difference between our method of convolution of the magnetization and C&P's method in terms of cubic spline. The magnetization after deconvolution for the noise level of  $1.5 \times 10^{-5} \text{ Am}^2$ , which is not so far from  $9.1 \times 10^{-6} \text{ Am}^2$ , were not disturbed by high frequency noise and are similar to the *ABIC* deconvolution result and the original magnetization. The difference of the solutions near the noise level of  $1.0 \times 10^{-5} \text{ Am}^2$  is critical and it can be said that careful noise estimation is indispensable for C&P's program.

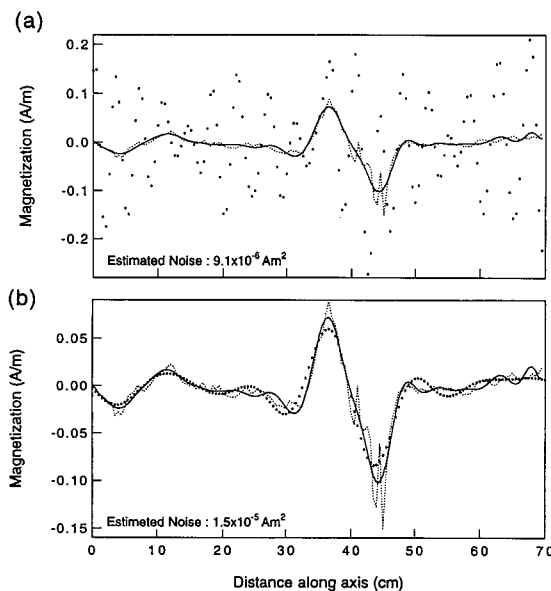


Fig. 8. Synthesized data with S/N ratio of 100 deconvolved using the program by Constable and Parker (1991). The magnetizations for estimated noise levels of (a)  $9.1 \times 10^{-6} \text{ Am}^2$  and (b)  $1.5 \times 10^{-5} \text{ Am}^2$  (solid circles) are shown with the magnetization of *ABIC* deconvolution (solid lines) and the magnetization of thin sections (broken lines).

Table 2. Noise levels and corresponding root mean squares (rms) of residuals between the deconvolved magnetization obtained for the program by Constable and Parker (1991) and the original magnetization.

noise ( $\text{Am}^2$ )	rms (A/m)
$9.1 \times 10^{-6}$	0.0963
$1.0 \times 10^{-5}$	0.0120
$1.5 \times 10^{-5}$	0.0117
$2.0 \times 10^{-5}$	0.0120
$4.0 \times 10^{-5}$	0.0130
$8.0 \times 10^{-5}$	0.0153

Table 3. Statistical parameters at minimum *ABIC* for the results of deconvolution on natural data for each of the three axes.

Axis	minimum <i>ABIC</i>	$\ln u$	rms of signal ( $\text{Am}^2$ )	rms of residuals ( $\text{Am}^2$ )	estimated S/N ratio
X	-4325.8	-3.00	$9.1 \times 10^{-4}$	$1.8 \times 10^{-5}$	51
Y	-4331.5	-4.00	$1.9 \times 10^{-3}$	$1.6 \times 10^{-5}$	120
Z	-4917.5	-4.50	$3.7 \times 10^{-4}$	$4.5 \times 10^{-6}$	82

The advantage of our method is that the optimum solution can be obtained objectively without any noise estimation, whereas the method by C&P is open to the risk of obtaining an unstable solution caused by underestimation of the noise level.

### 5.2 Real data

The magnetization obtained from the deconvolution of the whole-core data agreed well with natural remanent magnetization measured on the thin sections in each axis and revealed finer variation of the magnetization than the whole-core data. The convolution of NRM of thin sections are slightly lower than for the corresponding whole-core measurements. The lowering of NRM intensity of thin sections by drying (Otofujii *et al.*, 1982) and/or weight loss by slicing could be responsible for this.

The real data for X-axis also was deconvolved using the C&P's program and was compared with our result (Fig. 9). The estimated noise level of  $2.5 \times 10^{-5} \text{ Am}^2$  are used for C&P's program, because the estimated noise level of  $1.8 \times 10^{-5} \text{ Am}^2$ , which corresponds to rms of residuals of our *ABIC* deconvolution (Table 3), was too small to stabilize the solution. Deconvolved magnetization by our *ABIC* minimization method (Fig. 9(a), solid line) and C&P's method (Fig. 9(a), broken line) agreed very well. The residuals calculated by subtracting original magnetic moment from convolution of magnetization after deconvolution for *ABIC* minimization (solid line) and C&P's method (broken line) also show good agreement.

Residuals of raw data for our *ABIC* deconvolution showed sinusoidal fluctuations (Figs. 5(c), 6(c), 7(c)) for all three components, and was also hold on the residuals for C&P's method (Fig. 9(c)). The wave length is about 17 cm for the X and Y components, and 10 cm for the Z component. These wave lengths are nearly the same as the half-widths of the corresponding sensor response functions. A sinusoidal pattern was not observed in the residuals of synthesized data. We supposed that the sinusoidal fluctuations come from the difference in shape or half-width between true response and measured response curves. In order to test this, the synthesized data were deconvolved by using the synthesized sensor response function with a 1 cm-narrower half-width. The residuals for the results deconvolved by the true response function have a Gaussian distribution (Fig. 10(a)), whereas the residuals for the narrowed response function are modulated

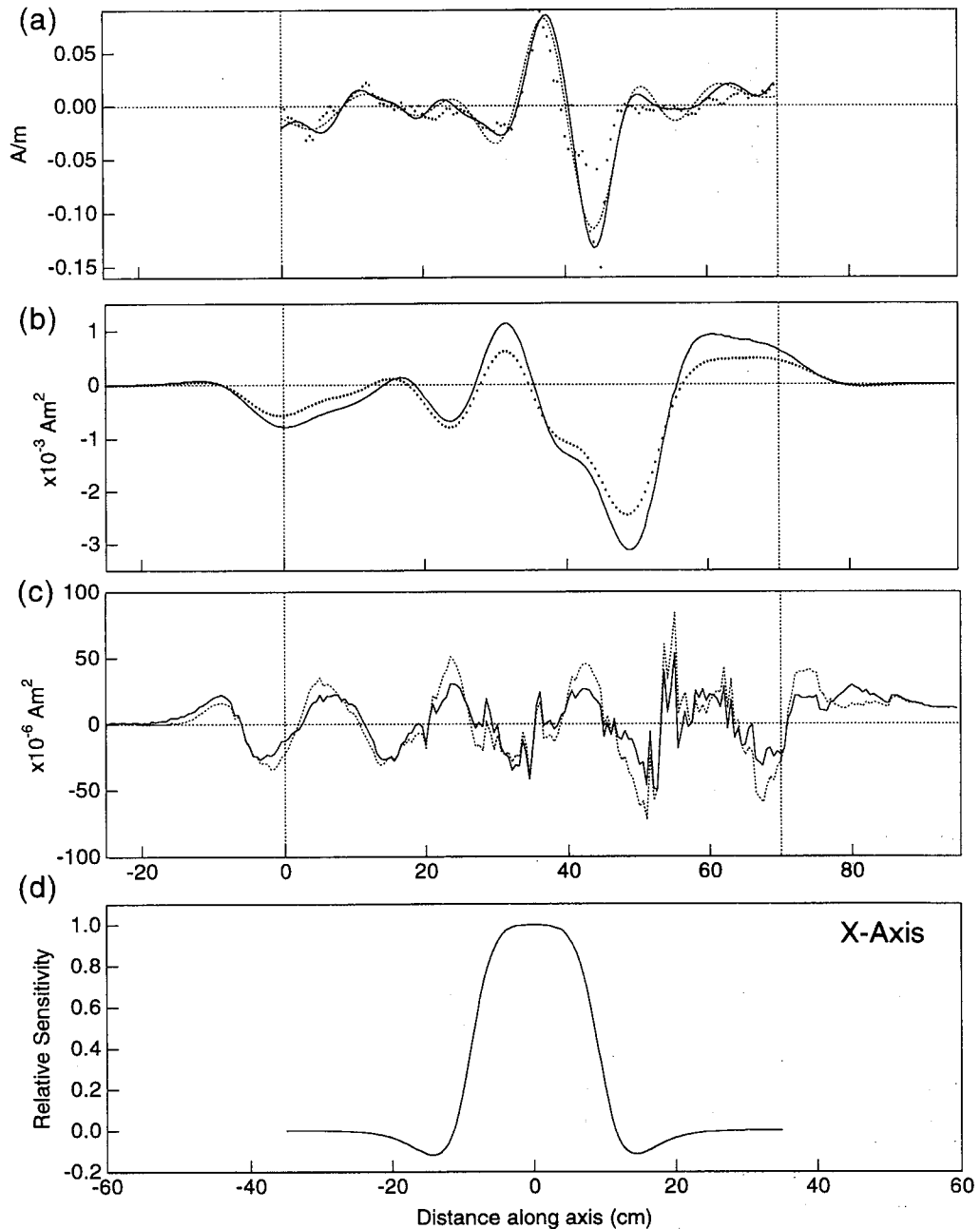


Fig. 9. Deconvolution of the X-component of magnetization for the "U-channel" sample by *ABIC*-minimizing method and C&P's method. The vertical broken lines correspond to the ends of the sample. (a) Magnetization after deconvolution of whole-core data by *ABIC* minimization (solid line) and C&P's method (broken line), and magnetization measured directly on thin sections (dots). (b) Pass-through measurement data (solid line) and convolution of NRMs of thin sections (dots). (c) Plot of residuals calculated by subtracting original magnetic moment from convolution of magnetization after *ABIC*-minimizing deconvolution (solid line) and C&P's deconvolution (broken line). (d) Normalized sensor response curve for X-axis. All the data points were measured at intervals of 5 mm.

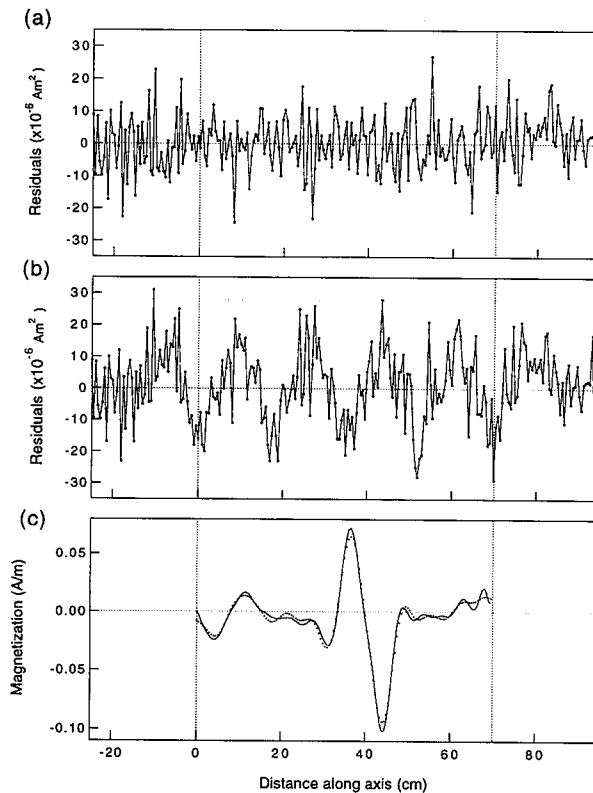


Fig. 10. Residuals of the total moment from the model moment for the results of deconvolution on synthesized data with S/N ratio of 100 by (a) the true sensor response curves, and (b) the response function of 1 cm narrower half-width. Residuals for narrowed response function show the characteristic wave length of about 18 cm. (c) Deconvolved magnetization using the true sensor response (solid line) and narrowed sensor response (dots).

by a wave length of about 18 cm, which is nearly the same pattern as the residuals for the raw data (Fig. 10(b)). This result suggests that the sinusoidal fluctuations in the residuals of the raw data can be attributed to the difference in half-width of the sensor response functions. The geometrical difference of cross section between the measured sample and the standard sample may be a cause of the difference in half-width of the sensor responses. The magnetizations deconvolved using the narrower sensor response showed nearly the same result as the former one, but were different in detail less than 5 cm wave length (Fig. 10(c)).

As pointed out by Constable and Parker (1991), the resolution of deconvolved magnetization cannot be significantly improved by reducing the measurement spacing. The noise level is one of the important factors controlling the resolution of the deconvolution. Table 3 shows statistical values where *ABIC* is a minimum for each axis. The rms of the whole-core data is  $9.1 \times 10^{-4}$ ,  $1.9 \times 10^{-3}$ , and  $3.7 \times 10^{-5}$   $\text{Am}^2$  for the X, Y and Z axis, respectively. The root sum square of differences between original whole-core data and convolution of calculated magnetization was  $1.8 \times 10^{-5}$ ,  $1.6 \times 10^{-5}$ , and  $4.6 \times 10^{-6}$   $\text{Am}^2$ . From these values, S/N ratios are calculated as 51, 120, and 82, respectively.

One of the noise sources of the measured data is inhomogeneity of the sample. The electromagnetic noise level of the cryogenic magnetometer is designed as  $5 \times 10^{-11}$ , for X and Y axes,



and  $3 \times 10^{-11} \text{ Am}^2$  for Z axis, which are much lower than the rms of residuals (Ishige *et al.*, 1989). Thus the main cause of inaccuracy in the deconvolution was not electromagnetic noise. We can estimate the total drift of the magnetometer (about  $10^{-6} \text{ Am}^2$  over 25 minutes) for the noise source from the whole-core measurement by comparing the magnetic moment beyond the region of the core. The drift of the X-component was the largest among the three axis. We did not take the drift component into account in the whole-core data.

A serious source of error is inaccuracy in sample positioning during measurement. The resulting error is the product of the magnetization gradient (typically  $\sim 10^{-5} \text{ Am}^2/\text{mm}$ ) and the departure from the expected position ( $\sim 1 \text{ mm}$  on average). Thus, the noise level coming from positioning inaccuracy is of the order of  $10^{-5} \text{ Am}^2$  and is nearly the same as the magnitude of the rms of residuals listed in Table 2. The noise may be significantly lowered by setting samples more accurately.

## 6. Conclusions

An objective deconvolution scheme was developed on the basis of Bayesian statistics. The deconvolution was performed as a smoothness-stabilized least squares method with optimum smoothness being determined by *ABIC* minimization. The deconvolution of synthesized data revealed finer variations of magnetization as the S/N ratio became higher. The *u* value that minimizes *ABIC* is close to the value that minimizes the residuals between model magnetization and deconvolved magnetization.

The magnetization obtained by the *ABIC*-minimizing deconvolution of whole-core data from a "U-channel" sample and that of thin sections cut from the same sample showed good agreement in three axes.

In the deconvolution scheme presented here, it is assumed that the magnitude of each component changes smoothly and magnetization is homogeneous in each unit slice. Although our deconvolution scheme does not always give the adequate results and needs to be improved. Bayesian deconvolution has the advantage that the optimum model can be selected from several different models with different parameters by simply minimizing *ABIC*. Thus, it will be easy to develop more realistic models for deconvolution.

We thank Akira Hayashida for permitting us to use a whole-core cryogenic magnetometer at Doshisha University; Dean Merrill of Texas A&M University for his kindness to take the "U-channel" sample; Masayuki Torii for his valuable advises on sample preparations and whole-core measurements; and the Constable and Parker for permitting us to use their deconvolution program. The sample was supplied with the permission of the Ocean Drilling Program. We are indebted to Dr. Charlie Barton and Dr. Phil McFadden at the Australian Geological Survey Organization, and an anonymous reviewer for their critical comments. This study was supported by the Grant-in-Aid for Specially Promoted Research No. 04216105 and the Grant-in-Aid for JSPS Fellows No. 1107 from Ministry of Education, Science, and Culture of Japan.

## REFERENCES

- Akaike, H., Likelihood and the Bayes procedure, in *Bayesian Statistics*, edited by J. M. Bernardo, M. H. Degroot, D. V. Lindley, and A. F. M. Smith, pp. 143-166, Univ. Press, Valencia, Spain, 1980.
- Constable, C. and R. Parker, Deconvolution of long-core palaeomagnetic measurements—spline therapy for the linear problem, *Geophys. J. Int.*, **104**, 453-468, 1991.
- Dodson, R., M. Fuller, and W. Pilant, On the measurement of the remanent magnetism of long cores, *Geophys. Res. Lett.*, **1**, 185-188, 1974.
- Ishige, T., A. Wakusawa, and K. Fujioka, Cryogenic system for the SQUID rock magnetometer, in *Proceedings of Third Japanese-Sino Joint Seminar on Refrigerators and Related Topics*, 13-16pp., The Cryogenic Society of Japan, Okayama, Japan, 1989.

- Murata, Y., Estimation of Bouguer reduction density using ABIC minimization method, *Seismology*, **43**, 327-339, 1990 (in Japanese).
- Otofujii, Y., I. Katsura, and S. Sasajima, Decay of a post depositional remanent magnetization in wet sediments due to the effect of drying, *Geophys. J. R. astr. Soc.*, **70**, 191-203, 1982.
- Rangin, C., E. A. Silver, M. T. von Breyman, *et al.*, *Proc. ODP, Init. Repts.*, **124**: College Station, TX (Ocean Drilling Program), 1990.
- Tamura, Y., T. Sato, M. Ooe, and M. Ishiguro, A procedure for tidal analysis with a Bayesian information criterion, *Geophys. J. Int.*, **104**, 507-516, 1991.
- Tauxe, L., J. L. Labrecque, R. Dodson, and M. Fuller, A new technique for paleomagnetic analysis of hydraulic piston cores, *EOS*, **64**, 219, 1983.